Evapotranspiration Modeling in ECHSE: Documentation

Julius Eberhard

May 26, 2017

Contents

1 Introduction

This is a documentation of my work done in exploring some aspects of the way how evapotranspiration is simulated in the *Eco-Hydrological Simulation Environment* (ECHSE, Kneis 2015) with methods, classes, and engines written by Tobias Pilz. ECHSE is a model framework, i.e. a software providing calculation methods that can be composed modularly to form model engines. These engines can be compiled and be run as independent models with input data. ECHSE is used in the field of (eco-) hydrology and therefore comes with a collection of methods especially relevant for issues in this field. The goal of the bigger project is to apply with ECHSE different models for determining the potential (et_{pot}) and the actual evapotranspiration (et_{act}). These are, as of the date of this documentation:

- the model of Makkink (1957),
- the model of Penman and Monteith (Monteith, 1965),
- the model of Penman and Monteith as simplified by the FAO (Allen et al., 1998),
- the model of Shuttleworth and Wallace (1985).

The engine-specific names (identifiers) of variables and parameters are written in `fixed-width` whereas the physical symbols of variables, constants, and parameters are written in *italics*. E.g., extraterrestrial radiation = R_{ex} = `radex`. Terms that describe parts of the ECHSE architecture are written in sans-serif.

1.1 Overview of models, engines, parameters

Models. The physical *et* models implemented in ECHSE originated from two approaches: First, the empirical approach of Makkink (1957) as simplified by De Bruin (1987) (for applications during the growing season) uses global radiation (explicitly), air pressure (implicitly through the use of the psychrometric 'constant'), and temperature (implicitly through the use of the slope of the saturated vapor pressure curve and the psychrometric 'constant') as predictors for the potential evapotranspiration. Secondly, the consideration of the net energy available for evaporating water from an open water surface was incorporated into earlier empirical findings by Penman and supplemented with the concept of surface and aerodynamical resistances for uniformly vegetated and completely covered ground by Monteith (1965) to form the Penman-Monteith model. For a nice overview of the Makkink (Makk) and the Penman-Monteith (PM) model and how they are theoretically related, see De Bruin (1987).

The widely used PM formula was later simplified for rough estimates of single crops by the Food and Agriculture Organization of the United Nations FAO (Allen et al., 1998) (FAO model) and improved for sparse crops by Shuttleworth and Wallace (1985) (SW model).

Tab. 1.1 gives a very brief overview of the four models. It contains keywords describing the way how a type of *et* is simulated in the respective ECHSE engine. *Reference et* quantifies the evapotranspiration from reference surfaces which usually are made of densely growing, clipped grass which always has a sufficient water supply for transpirating at a maximum rate. *Potential et* is the maximum possible evapotranspiration from a certain (not necessarily reference) surface which also has no limited water supply. *Actual et* takes into account factors that limit the water supply. E.g., potential *et* in the Makk model is calculated by multiplying the reference *et* with a crop factor while the potential *et* is multiplied with a soil moisture factor for determining the actual *et*.

Engines. All possibilities regarding the type of evapotranspiration (potential or actual), the model (Makk, PM, FAO, or SW), and other calculation methods are generally included in one engine. The engine requires the user to choose between the possible combinations of methods and follows them through the calculation process. Thus it is possible to directly compare the outputs of different methods with the same set of parameters which is supplied by the user.

Table 1.1: Overview of *et* models.

Model	Reference *et*	Potential *et*	Actual *et*
Makk	Makkink formula	× crop factor	× soil moisture factor
PM	—	PM formula, resistances w/o stress factors	PM, res. w/ stress
FAO	FAO formula	× crop factor	× soil moisture factor
SW	—	SW formula, resistances w/o stress factors	SW, res. w/ stress

Parameters. The engine parameters can be grouped into

- aerodynamic parameters,
- geographical parameters,
- radiation parameters,
- soil hydraulic parameters,
- vegetation parameters,

according to their physical role, and will be discussed in this order in Ch. 3. Within the ECHSE engines, parameters are grouped into the types

- paramNum (object-specific scalar parameters),
- sharedParamNum (group-specific scalar parameters),
- inputExt (group-specific time-dependent scalar parameters treated as external input variables),

according to their role in the computation process. Tab. 1.2 contains an overview of the variables and parameters and whether they are used in the different *et* models. The parameters in this overview are grouped into the types paramNum, sharedParamNum. Parameters of the inputExt type can be found together with the actual external input variables.

In Ch. 7, an overview of the estimated parameter values is given, grouped into the paramNum, sharedParamNum, and inputExt parameter types.

1.2 Study areas – available data

1.2.1 Portugal

The *Machoqueira do Grou* area is a 2,500 ha sized woodland in the Santarém district, between the towns of Coruche and Foros do Arrão, Portugal. The vegetation is dominated by cork oak trees and grasses. A part of the data comes from two measurement stations within the woodland, which were set up for recording eddy covariance data with measurement towers and other meteorological variables. One station is located between trees under the open sky (*Hauptstation*, HS), the other was set up under a cork oak (*Nebenstation A*, NSA). The data for both stations include

- net total radiation,
- air temperature,
- soil moisture content,
- sensible heat flux,
- latent heat flux,
- vapor pressure deficit,
- vapor pressure,
- wind speed;

they were recorded hourly. An evaporation flux was determined through the use of the Bowen ratio (→ Taylor & Ashcroft).

Additional meteorological data come from a nearby weather station. They include

- photosynthetically active radiation (PAR),
- incoming short-wave radiation,

– outgoing long-wave radiation,
– air temperature,
– relative humidity,
– rainfall,
– atmospheric pressure;

they were recorded half-hourly.

1.2.2 Morocco

The study area is a citrus orchard near the village Ait Cheikh, southwest of Marrakesh, lying in the Haouz plain north of the Atlas mountains (Mroos, 2014). The available data contain

– relative humidity,
– global radiation,
– air temperature,
– wind speed,
– latent heat;

they were recorded (latent heat: calculated?) half-hourly. An evaporation flux was determined from energy balance considerations.

Additionally, soil data were taken from Mroos (2014).

Table 1.2: External input variables, parameters and their usage in the *et* models. For abbreviations, see text. •: required by engine primarily, ○: required only in cases when some primary input is missing.

et_{pot}				et_{act}			
Makk	PM	FAO	SW	PM	FAO	SW	ECHSE identifier
							inputExt
	○	○	○				alb
•	•	•	•				apress
	•		•				cano_height
○	○	○	○				cloud*
○	○	○	○				doy
•	•	○	•				glorad
	○	○	○				glorad_max
○	○	○	○				hour
	•		•				lai
	○	○	○				rad_long
	•	•	•				rad_net
	○	○	•				rad_net_soil
	•	•	•				rhum
	•		•				soilheat
○	○	○	○				sundur
○	○	○	○				temp_max
○	○	○	○				temp_min
•	•	•	•				temper
			•				totalheat
○	○	○	○				utc_add
							wc_vol_root
							wc_vol_top
	•	•	•				wind
							paramNum
	•		•				bubble
		•					crop_faoref
•							crop_makk
○	○	○	○				elev
	•		•				glo_half
○	○	○	○				lat
	○	○	○				lon
				•		•	par_stressHum
				•		•	pores_ind
	•		•				res_leaf_min
			•				soil_dens
							wc_etmax
							wc_pwp
							wc_res
							wc_sat
							wstressmax
							wstressmin
							sharedParamNum
•	•	•	•				choice_et
	○	○	○				choice_gloradmax
	•		•				choice_plantDispl
	•		•				choice_rcs
	•		•				choice_roughLen
	•		•				drag_coef
			•				eddy_decay
	○	○	○				emis_a
	○	○	○				emis_b
	•		•				ext
	○	○	•				f_day
	○	○	•				f_night
	○	○	○				fcorr_a
	○	○	○				fcorr_b
	•						h_humMeas
	•						h_tempMeas
	•	•	•				h_windMeas
○	○	○	○				radex_a
○	○	○	○				radex_b
			•				res_b
	•		•				rough_bare
			•				rss_a
			•				rss_b
							**currently not used*

2 Aims

The aims of my work are:

- the estimation of engine parameters through transfer functions and model calibration (Ch. 3),
- comparison of the different evapotranspiration models (Ch. 4),
- sensitivity analysis of engine parameters (Ch. 5),
- evaluation of single methods employed in the *et* models (Ch. 6).
- Which input data do we still need? (Ch. 8)

3 Parameters: methods and results

The estimation of **aerodynamic parameters**, which specify the aerodynamic resistances in the PM and the SW models, was mostly not possible in the study cases and therefore adopted from the original publications. Nevertheless, the origins of the values are discussed briefly (Sec. 3.1).

Geographical parameters were given or easy to estimate from map services (Sec. 3.2).

Radiation parameters were partly estimated from observations of radiation components at the study sites and are discussed more extensively (Sec. 3.3).

Two pedotransfer functions (PTF) were used to estimate **soil hydraulic parameters** from the measured soil properties, namely bulk density, mass portions of silt and clay, and organic matter content (Sec. 3.4).

All **vegetation parameters** were adapted from other publications or estimated through model calibration (Sec. 3.5). They are discussed in separate sections to specify the problems and possibilities relevant for their determination.

Where parameters appear in their own sections, the discussion follows the outline *Basics – Methods – Notes – Portugal – Morocco*.

3.1 Aerodynamic parameters

All estimated or adopted values were employed for both Portugal and Morocco because the aerodynamic conditions are similar.

Below the canopy toward the ground, wind speed is assumed to decrease exponentially with a scaling coefficient n, called the **eddy diffusivity decay constant** (`eddy_decay`); more precisely: The shearing stress of wind on a horizontal plane is proportional to $\rho \partial u / \partial z$ (where u is the horizontal wind component, z the vertical coordinate, and ρ the density of air) with the proportionality factor K. n relates the magnitude of K at the canopy height to that at the ground. Shuttleworth and Wallace (1985) use a value of $n = 2.5$, arguing that it results from the crop specification made by Monteith (1973) in deriving the above relation. Although I couldn't reconstruct this value from the second edition of Monteith's book (Monteith, 1990), Shuttleworth and Wallace (1985) concluded from an sensitivity analysis that the resulting evapotranspiration was hardly influenced by changing n. Therefore, n has been set to 2.5.

The **measurement heights of relative humidity** (`h_humMeas`), **temperature** (`h_tempMeas`), and **wind speed** (`h_windMeas`) are known from the measurement setups and each equal to 2 m in Portugal as well as in Morocco.

The aerodynamic **mean boundary layer resistance** r_b (`res_b`) was taken as 25 s m^{-1} by Shuttleworth and Wallace (1985) based on field measurements by Denmead (1976) and Uchijima (1976). Like for n, the models seem to be quite insensitive for variations of r_b (Shuttleworth and Wallace, 1985), and r_b has been set to 25 s m^{-1}.

In the calculation of the aerodynamic resistance between canopy and reference level, the displacement height of the vegetation and the roughness lengths for latent and sensible heat fluxes of the vegetation are used (see Sec. 3.5 for these parameters). Following Shuttleworth and Gurney (1990), both of these are dependent on the **roughness length of the bare substrate** z_0 (`rough_bare`) and the effective mean **drag coefficient of the vegetation** c_d (`drag_coef`) as well as on the leaf area index and the canopy height (Sec. 3.5). The values of z_0 and c_d were numerically estimated by the authors and are adopted here as 0.01 m and 0.07, respectively.

3.2 Geographical parameters

Each model employs 3 or less geographical parameters for calculating the radiation balance: **latitude** φ (`lat`), **longitude** L_m (`lon`), **elevation** h (`elev`). For the sites in Portugal, the locations were given as UTM coordinates (HS: 557,640.5 m easting, 4,332,523.5 m northing; NSA: 557,717.0 m easting, 4,332,408.0 m northing; both in UTM zone 29S) from which I could derive $\varphi = 39.14°$ N and $L_m = 8.33°$ W for both field stations. The actual distance of 139 m between the stations corresponds to less than 0.01° and was therefore taken as 0. A common value for h of the Portugal sites was estimated from local elevation maps (*floodmap.net*) as 160 m above sea level.

For Morocco, $\varphi = 31.50°$ N, $L_m = 8.14°$ W, and $h = 464$ m a.s.l. were taken from Mroos (2014).

3.3 Radiation parameters

3.3.1 Albedo (`alb`)

Basics. The albedo μ (`alb`) is defined as

$$\mu = \frac{R_{outS}}{R_{inS}}$$

with

R_{outS}: outgoing short-wave radiation, in W m^{-2},
R_{inS}: incoming short-wave radiation (`glorad`), in W m^{-2}.

Method. It can be estimated from observations of R_{inS} and R_{outS} or from literature values for various land surfaces. The albedo of a surface can change over time and is supplied as a time series in ECHSE.

Portugal. The measurements of the short-wave radiation components at the stations HS and NSA comprised hourly time series between April 7 and August 4, 2014. The albedo was derived as a total mean of the hourly R_{outS}/R_{inS} ratio. Only records of times between 8:00 and 16:00 were used for the estimation. Although the observations showed a distinct development over time (Fig. 3.1), I could not conclude the amplitude of yearly fluctuations from the observations and therefore used the calculated mean as a constant value over the whole year, $\mu = 0.066$.

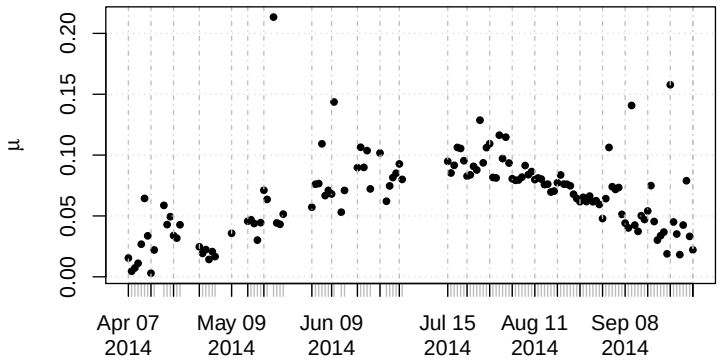

Figure 3.1: R_{outS}/R_{inS} ratio, daily mean. Total mean: $\mu = 0.0816$.

Morocco. None of the measurements did include R_{outS} data, so the albedo has been estimated as constantly 0.3, judging by the descriptions of the surfaces. These are likely to have $0.25 < \mu < 0.4$, where 0.25 is the albedo of green grass (Markvart and Castañer, 2003) and 0.4 that of dry sand (Tetzlaff, 1983).

3.3.2 Emissivity parameters (`emis_a`, `emis_b`)

Basics. Emissivity is a property of a macroscopic body (fluid or solid) and gives the portion of radiation that the body emits compared with a black body at the same temperature. There are two methods for calculating the net emissivity ε between Earth's surface and atmosphere in ECHSE, either from water vapor pressure (Eq. 3.1) or from air temperature (Eq. 3.3). The first method includes the emissivity parameters ε_a, ε_b (`emis_a`, `emis_b`), which represent the average environmental effects (such as surface and climate) on ε at a certain location (Brunt, 1932):

$$\varepsilon = \varepsilon_a + \varepsilon_b \sqrt{e} \tag{3.1}$$

with

ε: net emissivity, no unit,
ε_a: emissivity parameter a, no unit,
ε_b: emissivity parameter b, in $\mathrm{hPa}^{-1/2}$,
e: water vapor pressure in air, in hPa.

e is derived from measurements of the air temperature and the relative humidity. ε itself is used in ECHSE for the calculation of the net incoming long-wave radiation (adapted Stefan-Boltzmann law):

$$L_n = -f\varepsilon\sigma(TA + 273.15\ \mathrm{K})^4 \tag{3.2}$$

with

L_n: net incoming long-wave radiation, in $\mathrm{W\ m^{-2}\ K^{-4}}$,
f: cloudiness correction factor (Sec. 3.3.4), no unit,
ε: net emissivity between ground and atmosphere, no unit,
σ: Stefan-Boltzmann constant, $5.670373 \times 10^{-8}\ \mathrm{W\ m^{-2}\ K^{-4}}$,
TA: mean air temperature, in °C.

Method. The parameters ε_a, ε_b can be estimated through Eqs. (3.2) and (3.1) if sufficient data of L_n, TA, e, and f are available. If not, one can look up suggested values by Maidment (1993) (p. 4.7), i. e. $\varepsilon_a = 0.34$ and $\varepsilon_b = -0.14$ for "average conditions" and general ranges of 0.34 to 0.44 for ε_a and -0.14 to -0.25 for ε_b, derived from data in Doorenbos and Pruitt (1977).

Note. The second method for calculating ε uses air temperature as the only predictor for ε without the need of ε_a, ε_b, e and was derived in Maidment (1993) based on Idso and Jackson (1969):

$$\varepsilon = -0.02 + 0.261 \exp(-7.77 \times 10^{-4} TA^2) \tag{3.3}$$

It seems that Eq. (3.1) is the more suitable choice if e is known since it lets the user implement more of the specific environmental conditions at a study site through the emissivity parameters. However, if ε_a and ε_b can't be determined as explained and both e and TA data are available, the question is whether it is better to use Eq. (3.1) with average-condition values from Maidment (1993) or Eq. (3.3). ECHSE prefers Eq. (3.1) as soon as any e data are given as an input and thereby follows the recommendation of Maidment (1993). As can be seen in Sec. 3.3.4, the cloudiness correction factor f is determined by two parameters (f_a, f_b), which need to be supplied by the user. Their estimation is possible only through the use of Eq. (3.2), thus dependent on ε data. This means that a well-founded calculation of the emissivity is the requirement for a good estimation of f_a and f_b. Since it was not clear which method would provide a better value of ε, I decided to use both methods and compare the outputs of the models.

Portugal. I chose default values of $\varepsilon_a = 0.34$ and $\varepsilon_b = -0.14$, as suggested for average conditions by Maidment (1993). The values could not be estimated specifically because the cloudiness correction f was not known for the study site. Instead, f was estimated with the adopted emissivity parameters through Eq. (3.2) for the determination of the cloudiness correction parameters f_a, f_b. For a qualitative validation of the chosen values, I estimated the net emissivity from Eq. (3.2) using observations at times when global radiation was at maximum, i. e. $f \approx 1$, and compared it to the predicted values of

ε by both emissivity models. Fig. 3.2 shows "observed" and predicted ε values, distinguishing between "noon" hours (between 10 am and 2 pm), when L_n has a maximal magnitude, and other hours of the day. f was chosen to be $0.9 < f \leq 1$. Although some observation-derived values come near the predicted values at noon hours, both models seem to overpredict the "observed" emissivity.

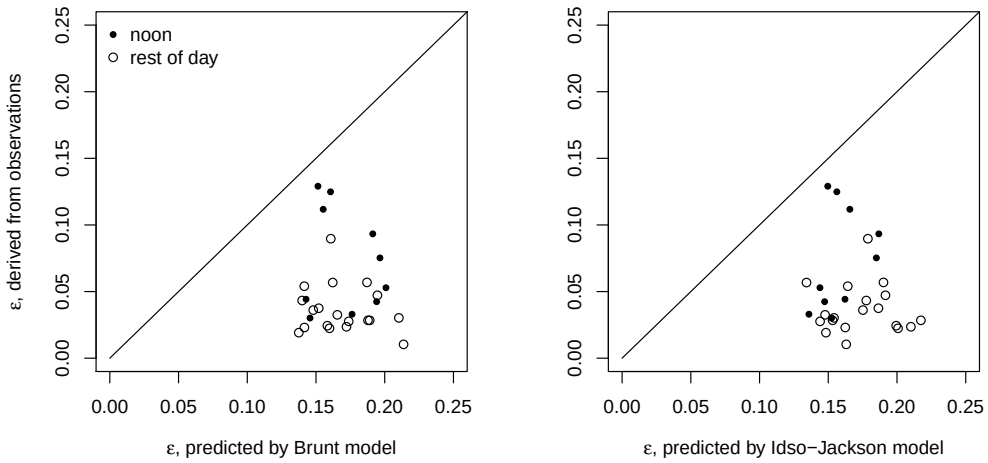

Figure 3.2: Observation-derived vs. model-predicted net emissivity. As $f \approx 1$ was assumed by choosing $0.9 < f \leq 1$, Eq. (3.2) is equivalent to $\varepsilon \approx -L_n/(\sigma(TA + 273.15\ \mathrm{K})^4)$ with observed L_n and TA.

Morocco. As for Portugal, I chose $\varepsilon_a = 0.34$ and $\varepsilon_b = -0.14$. The values could not be estimated specifically because data of the net long-wave radiation and the cloudiness correction were missing.

3.3.3 Soil heat factors (`f_day`, `f_night`)

Basics. Within the ECHSE engines, the sub-daily soil heat flux is currently calculated as

$$G_{soil} = f_{day} R_{net} \text{ during daytime,} \tag{3.4}$$

$$G_{soil} = f_{night} R_{net} \text{ during nighttime.} \tag{3.5}$$

with

G_{soil}: soil heat flux (`soilheat`), in W m^{-2},
f_{day}, f_{night}: soil heat factors (`f_day`, `f_night`), no unit,
R_{net}: net incoming short-wave and long-wave radiation (`rad_net`), in W m^{-2}.

Portugal. Since the data didn't include measurements of R_{net}, I used the results of internally calculated values of R_{net} and measurements of G_{soil} for calculating f_{day}, f_{night} hourly from Eqs. (3.4), (3.5). The distinction of the time series into daytime and nighttime was made using the *RAtmosphere::suncalc* procedure by Gionata Biavati, which provided sunrise and sunset times for the study site. Averaging over all hours gave the results.

Morocco. —

3.3.4 Cloudiness correction parameters (`fcorr_a`, `fcorr_b`)

Basics. The cloudiness correction parameters f_a, f_b (`fcorr_a`, `fcorr_b`) appear as the slope and the intersect parameter of the affine relationship between the cloudiness correction factor f and the relative actual global radiation:

$$f = f_a \frac{R_{inS}}{R_{inS,cs}} + f_b \tag{3.6}$$

with

f_a, f_b: cloudiness correction parameters, no unit,
R_{inS}: actual incoming short-wave radiation (`glorad`), in W m^{-2},
$R_{inS,cs}$: maximum possible ("clear-sky") incoming short-wave radiation, in W m^{-2}.

f itself is used in ECHSE for the calculation of the net incoming long-wave radiation, i.e. Eq. (3.2):

$$L_n = -f\varepsilon\sigma(TA + 273.15\ \mathrm{K})^4$$

with

L_n: net incoming long-wave radiation, in W m^{-2} K^{-4},
ε: net emissivity between atmosphere and ground (Sec. 3.3.2), no unit,
σ: Stefan-Boltzmann constant, 5.670373×10^{-8} W m^{-2} K^{-4},
TA: mean air temperature, in °C.

Method. The parameters can be estimated from Eq. (3.2) if sufficient data of L_n, ε, TA, R_{inS}, and $R_{inS,cs}$ are available. Shuttleworth gives values of $f_a = 1.35$, $f_b = -0.35$ for arid conditions and $f_a = 1.0$, $f_b = 0.0$ for humid conditions in Maidment (1993), p. 4.8.

Portugal. First, the cloudiness correction f was estimated from L_n, TA, and ε where the net emissivity was calculated following both methods described in Sec. 3.3.2, i. e. Eq. (3.1) (Brunt, 1932) and Eq. (3.3) (Idso and Jackson, 1969). The parameters f_a, f_b could then be estimated through an adapted regression method: The condition $f_a + f_b = 1$ was not possible to be fulfilled by a linear regression of f over $R_{inS}/R_{inS,cs}$ (the latter of which was derived by means of the previously estimated Ångström parameters). In order to get a model close to the data, I did a linear regression of the data (although the conditional mean didn't behave linearly and therefore did not fulfill the assumptions for a valid linear regression) and used the intersect (the value of f at $R_{inS} = 0$) as estimation of f_b. f_a was then determined from the condition above. Fig. 3.3 shows the calculated cloudiness correction and the adapted regression models for both emissivity methods as well as the suggested model by Shuttleworth in Maidment (1993).

Morocco. Data of the net long-wave radiation were missing, thus I chose the suggested values for arid conditions in Maidment (1993).

3.3.5 Ångström parameters (`radex_a`, `radex_b`)

Basics. The estimation of the Ångström parameters is based on the equation

$$\langle R_{inS}\rangle = \left(a_s + b_s\frac{n}{N}\right)\langle R_{ex}\rangle, \tag{3.7}$$

with

$\langle\cdot\rangle$: daily mean of $\cdot$,
R_{inS}: incoming short-wave radiation (global radiation, `glorad`), in W m^{-2},
R_{ex}: extraterrestrial short-wave radiation (`radex`), in W m^{-2},
a_s, b_s: Ångström parameters (`radex_a`, `radex_b`), no unit,
n: sunshine duration of current day (time for which $\langle R_{inS}\rangle \geq 120$ W m^{-2}, `sundur`), in hours,
N: maximum possible sunshine duration, in hours.

Method 1. Since R_{ex} and N are calculated internally and astronomically based, the uncertainty of the estimation through Eq. (3.7) should only depend on the observed global radiation (by definition, n follows from R_{inS}). Note that the equation as written represents only daily mean values of R_{inS}: The parameters are weighted depending on the daily ratio n/N in order to account for cloudiness. Two special cases are therefore

$$a_s + b_s = \frac{\langle R_{inS}\rangle}{\langle R_{ex}\rangle} \text{ on days when } n = N, \tag{3.8}$$

$$a_s = \frac{\langle R_{inS}\rangle}{\langle R_{ex}\rangle} \text{ on days when } n = 0. \tag{3.9}$$

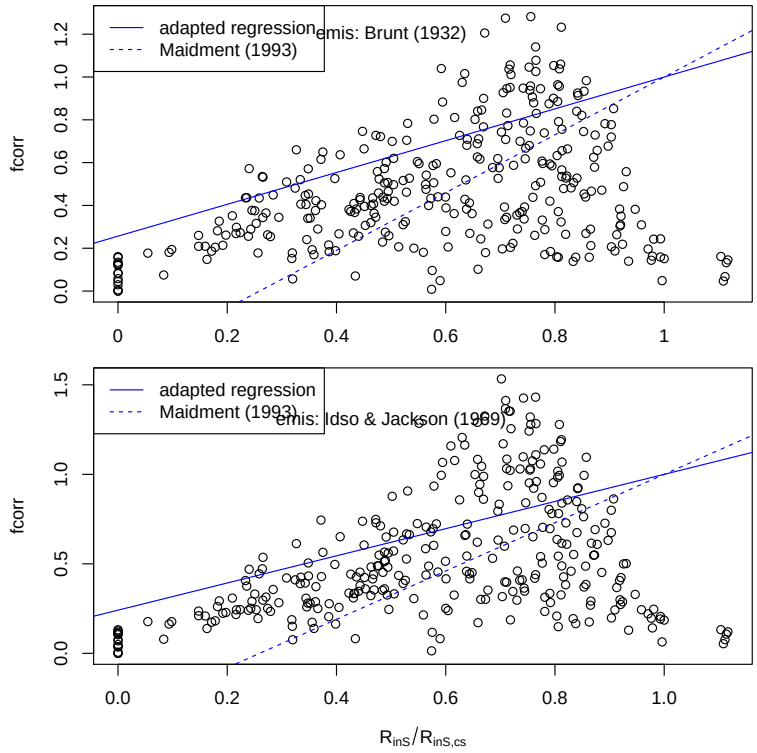

Figure 3.3: Adapted regression models (lines) of hourly f data (points) calculated with Eq. (3.2) for the estimation of f_a, f_b. See text for the regression method. Upper: emissivity calculated after Brunt (1932) with $\varepsilon_a = 0.34$, $\varepsilon_b = -0.14$; lower: emissivity calculated after Idso and Jackson (1969).

If observations for either of these cases are available, Eqs. (3.7) & (3.8) or Eqs. (3.7) & (3.9) form a system of linear equations, i.e. the unknown parameters a_s, b_s can be found for any given day with known values of n and R_{inS}. Averaging over all days would then determine the parameters. Problem: It might be difficult to find either days when $n = N$ or days when $n = 0$.

Method 2. Another way of estimating a_s and b_s based on shorter time intervals (in our case, hourly) would be

$$a_s + b_s = \max_{h=1,\ldots,24} \left\{ \frac{R_{inS}(h)}{R_{ex}(h)} \right\}, \tag{3.10}$$

$$a_s = \min_{h=1,\ldots,24} \left\{ \frac{R_{inS}(h)}{R_{ex}(h)} \right\} \tag{3.11}$$

with

h: hour of day.

For finding unique solutions, both Eqs. (3.10) and (3.11) need to be evaluated because the equations are no longer dependent on n. The biggest problem of estimating the parameters with subdaily data is that extreme values (max, min) can result from measuring errors and statistical outliers. Taking very low quantiles of the R_{inS}/R_{ex} distribution and applying an upper limit for the max ($a_s + b_s$ can't be greater than 1) would probably avoid estimating a_s as too low and b_s as too high.

Portugal. Global radiation was measured hourly at the local weather station in Portugal. Therefore I chose to estimate `radex_a` and `radex_b` with Eqs. (3.10) and (3.11). The R_{inS}/R_{ex} ratio was calculcated for daytime hours between 8:00 and 16:00 local time. This assured that only radiation between sunrise and sunset was taken into account for all of the simulation period. For the determination of reasonable values I chose the lower 5-percentile of the R_{inS}/R_{ex} distribution as the minimum and the maximum value of $\{R_{inS}/R_{ex} < 1\}$ as the maximum over the whole period in which R_{inS}

observations were available. These choices proved successful in computing clear-sky radiation that didn't exceed the observed global radiation and therefore fulfilled the physical conditions.

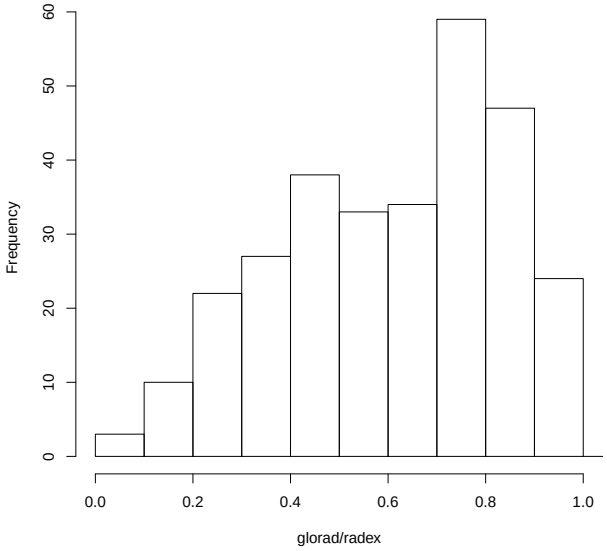

Figure 3.4: Histogram of the ratio R_{inS}/R_{ex} for values less than 1 in Portugal.

Morocco. —

3.4 Soil hydraulic parameters

`wc_sat`, `wc_res`, `wc_pwp`, `wc_etmax`, `bubble`, `pores_ind`, `wstressmin`, `wstressmax`, `soil_dens`, `rss_a`, `rss_b`.

3.4.1 Capillary suction at maximum/minimum water stress (`wstressmax` / `wstressmin`)

Basics. The calculation of stomatal resistance, which is required in the PM and SW models, incorporates two stress factors for vapor stress (Φ_{vap}) and water stress (Φ_{wat}). The latter one relates the actual capillary suction in the soil ψ to the capillary suction at maximum ($\psi_{s,max}$) and minimum water stress ($\psi_{s,min}$) and reads

$$\Phi_{wat} = \begin{cases} 1, & \psi < \psi_{s,min} \\ 1 - \frac{\psi - \psi_{s,min}}{\psi_{s,max} - \psi_{s,min}}, & \psi_{s,min} \leq \psi < \psi_{s,max} \\ 0.01 & \psi \geq \psi_{s,max} \end{cases}$$

with

ψ: actual capillary suction, in hPa,
$\psi_{s,max}$: capillary suction at maximum water stress (`wstressmax`), in hPa,
$\psi_{s,min}$: capillary suction at minimum water stress (`wstressmin`), in hPa.

Method. Since water stress for a plant is at maximum when it is not able to detract water from the soil anymore, it's a plausible decision to set $\psi_{s,max}$ to the defined (Scheffer and Schachtschabel, 2010) permanent wilting point of $10^{4.2}$ hPa. $\psi_{s,min}$ is more difficult to determine but simple sensitivity analyses showed almost no influence of a variation of $\psi_{s,min}$ between 0 and 500 hPa (a range from full saturation to above the upper range of field capacity at $10^{2.5}$ hPa) on the simulated actual evapotranspiration.

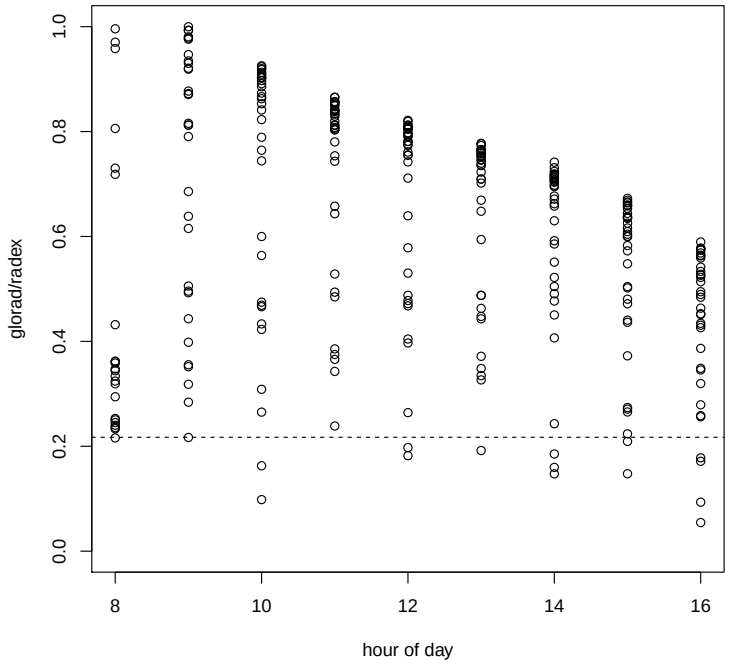

Figure 3.5: R_{inS}/R_{ex} ratio dependent on hour of day. The shift of higher values toward early hours may indicate either a small temporal deviation between the simulated and the actual R_{ex}, or a local effect that weakens R_{inS} during afternoon, or both. The dashed line marks the 5-percentile of the total distribution.

Portugal, Morocco. Following the explanations above, I set $\psi_{s,max} = 15849$ hPa $\approx 10^{4.2}$ hPa and $\psi_{s,min} = 100$ hPa.

3.5 Vegetation parameters

3.5.1 Canopy height (`cano_height`)

Basics. In the calculation of different aerodynamic resistances, the average canopy height of the vegetation h_{cano} (`cano_height`) is an important parameter. The dependent quantities include, among others, the displacement height and the roughness length of the vegetation.

Method. The canopy height can be measured in situ or estimated species- and climate-dependently from literature.

Portugal. At HS, the predominant species are grasses for which I assumed a mean canopy height of 0.20 m. At NSA, the total heights of the surrounding trees were measured. The mean is 7.98 m for a sample size of 88 and was used as canopy height.

3.5.2 FAO crop factor (`crop_faoref`)

Basics. The modified Penman-Monteith formula as published by the FAO (Allen et al., 1998) gives a rough estimation of the potential evapotranspiration rate without the explicit use of resistances but empirically generalized factors. The FAO crop factor (`crop_faoref`), which scales the total *et* flux, is the only parameter in the equation and specific to a site, i.e. a crop. A value of 1 corresponds to the reference crop (well-watered grass of 0.12 m height, 70 s m^{-1} (Allen et al., 1998) or 69 s m^{-1} (Shuttleworth, 2007) surface resistance, 0.23 albedo), values for other types of vegetation can be looked up online.

Portugal, Morocco. The crop factor was set to 1 for reference evapotranspiration. Since the FAO equation is just a simplification of the Penman-Monteith equation, I preferred using the original PM model for the study cases and using the FAO reference results only for a subsumption of the different models.

3.5.3 Makkink crop factor (`crop_makk`)

Basics. The Makkink model expresses a simple empirical relationship between the global radiation, the air temperature, and the potential evapotranspiration of a crop. The type of crop is regarded in terms of the Makkink crop factor (`crop_makk`), which scales the *et* flux compared to that of a reference crop (well-watered grass of 0.08–0.13 m height, Feddes 1987).

Method. It was estimated from the leaf area index (Sec. 3.5.7) by the affine relation

$$\text{Makkink crop factor} \approx 0.14\ LAI + 0.4 \tag{3.12}$$

with

LAI: leaf area index, in $\mathrm{m}^2\ \mathrm{m}^{-2}$.

This relation was derived in the ECHSE documentation from data of Feddes (1987) and Ludwig and Bremicker (2006).

Portugal.

Morocco.

3.5.4 Extinction coefficient (`ext`)

3.5.5 Radiation for half-maximum stomatal conductance (`glo_half`)

Basics. When using the PM or SW model, the modeler is interested in the bulk surface resistance of a canopy, r_{cs}, which is practically not measurable. ECHSE provides two ways of calculating r_{cs} from the stomatal resistance of a single average leaf, which is measurable. If the user decides to use the formula of Saugier and Katerji (1991), the incoming short-wave radiation at which the stomatal conductance is half of its maximum (g_{srad}, `glo_half`) will be needed. In their derivation of the formula, the authors assume that the actual stomatal resistance of a leaf is hyperbolically dependent on the incident short-wave radiation,

$$r_{l,act} = r_{l,min}\frac{R_{inS} + g_{srad}}{R_{inS}} \tag{3.13}$$

with

$r_{l,act}$: actual stomatal resistance of one leaf, in $\mathrm{s\ m}^{-1}$,
$r_{l,min}$: minimum stomatal resistance of one leaf, in $\mathrm{s\ m}^{-1}$,
R_{inS}: incoming short-wave radiation, in $\mathrm{W\ m}^{-2}$,
g_{srad}: short-wave radiation for half-maximum stomatal conductance, in $\mathrm{W\ m}^{-2}$,

which is justified because the opening of stomata is known to be due to increasing light (Sonnewald, 2013). They assume also that the radiation inside or under the canopy decreases exponentially as $R_{inS}\exp(-\epsilon LAI)$ with the extinction coefficient ϵ (Sec. 3.5.4), no unit, and the leaf area index LAI (Sec. 3.5.7), no unit. After integrating $r_{l,act}$ over all leaves, the resulting formula reads

$$r_{cs} = \epsilon r_{l,min} / \ln\frac{\epsilon R_{inS} + g_{srad}}{\epsilon R_{inS}\exp(-\epsilon LAI) + g_{srad}}. \tag{3.14}$$

Method. The parameter of interest, g_{srad}, can be determined by measurements of the stomatal conductance/resistance of multiple leaves over a broad range of radiation conditions and is assumed to be specific of a species. Saugier and Katerji (1991) collected some values,

– alfalfa: 180 $\mathrm{W\ m}^{-2}$ (Katerji et al., 1983),

– sunflower: 200–350 W m^{-2} (Berger, 1973),
– Scots pine: 125 W m^{-2} (Lohammar et al., 1980) and 150 W m^{-2} (Jarvis and Morison, 1981),
– apple tree: 50 W m^{-2} (Warrit et al., 1980),
– oil palm: 30 W m^{-2} (Dufrêne, 1989),

which I used for the estimation of g_{srad} through model calibration (?).

Note 1. Since conductance is equal to inverse resistance, g_{srad} corresponds to the global radiation at which the stomatal *resistance* is double of its minimum value.

Note 2. The described approach of Saugier and Katerji (1991) was basically applied in the WASA model for semi-arid conditions (Güntner, 2002) and is implemented in ECHSE. In both cases the minimum resistance of a single leaf in Eq. (3.14) was replaced by the actual resistance of a single leaf, $r_{l,act}$. This adaption is justified because $r_{l,act}$, as used in WASA and ECHSE, represents the minimum stomatal resistance regarding all other factors than radiation, which was used as $r_{l,min}$ by Saugier and Katerji (1991) for their derivation of Eq. (3.14).

Note 3. The other method for r_{cs}, from Shuttleworth and Wallace (1985), uses the leaf area index as the only predictor. It is discussed in the next section since two different versions of the equation exist in the literature.

3.5.6 Note on the calculation of the canopy resistance r_{cs}

Instead of using Eq. (3.14) from Saugier and Katerji (1991), the canopy stomatal resistance r_{cs} can be estimated simply from the stomatal resistance of a single average leaf in the canopy and the leaf area index (Sec. 3.5.7). Shuttleworth (1976) showed that the canopy stomatal resistance is inversely proportional to the leaf area index and postulated the following relationship for a canopy of amphistomatous leaves (e.g. some grasses or conifers, Shuttleworth and Wallace 1985):

$$r_{cs} = \frac{\overline{r_{l,act}}}{2LAI} \tag{3.15}$$

with

r_{cs}: canopy stomatal resistance, in s m^{-1},
$\overline{r_{l,act}}$: actual stomatal resistance of a single average leaf.

The factor 1/2 might come from the consideration of both sides of an amphistomatous leaf when calculating the canopy resistance whereas the resistance of a single leaf is usually measured for one side only. However, this is my personal conjecture.

The other version of the above relationship (Eq. 3.15) is

$$r_{cs} = \frac{\overline{r_{l,act}}}{LAI_{active}} = \frac{\overline{r_{l,act}}}{0.5LAI} \tag{3.16}$$

and was published by the FAO (`www.fao.org/docrep/X0490E/x0490e06.htm`, Box 5) as an estimate for a reference crop, i.e. clipped, dense-growing grass where only the upper half of the canopy – expressed as active leaf area index LAI_{active} – is considered to contribute to mass and heat transport toward the atmosphere (Allen et al., 1998). The underlying assumption in Eq. (3.16) apparently takes into account only one side of the leaves. This estimate of a reference canopy resistance was used in the SWAT model.

ECHSE currently employs the "original" version of Shuttleworth and Wallace (1985) (Eq. 3.15) and there is no good reason yet to use Eq. (3.16) instead. (Sensitivity?)

3.5.7 Leaf area index (`lai`)

Basics. Especially in estimating surface resistances of the vegetation and other vegetation parameters, the leaf area index LAI (`lai`) plays an important role. It is the average one-sided area of all leaves of a plant that grow above one square meter of the ground.

Method. LAI can be measured in situ by collecting all plants from sample sites within the study area. Where direct measurements are difficult to realize, LAI can be estimated from data of plant allometry, usage of dry masses and specific leaf area indices, or light measurements.

Portugal. For both sites, LAI was measured at 25 sample sites within a square of 25 m side length. The results were 0.778 at HS and 1.397 at NSA.

Morocco. From the descriptions of the study area, a photograph, and a sketch of a part of the orchard (Mroos, 2014), I could estimate an average LAI. Jahn (1979) reported leaf area indices for single citrus trees between 3.7 and 15.1 with a mean of 8.8. Using this value for the citrus-covered area, a LAI of 0.5 for the sparsely grass-covered areas between the trees, and a tree cover portion in the area of roughly 0.3 (patterns with one tree of canopy radius 1.5 m per 6×4 m^2 plot), the estimated effective value is $LAI = 2.99$.

3.5.8 (par_stressHum)

Basics.

3.5.9 (res_leaf_min)

4 Comparison of evapotranspiration models

5 Sensitivity analysis

6 Evaluation of ECHSE methods

6.1 Global radiation glorad

6.1.1 glorad: Portugal

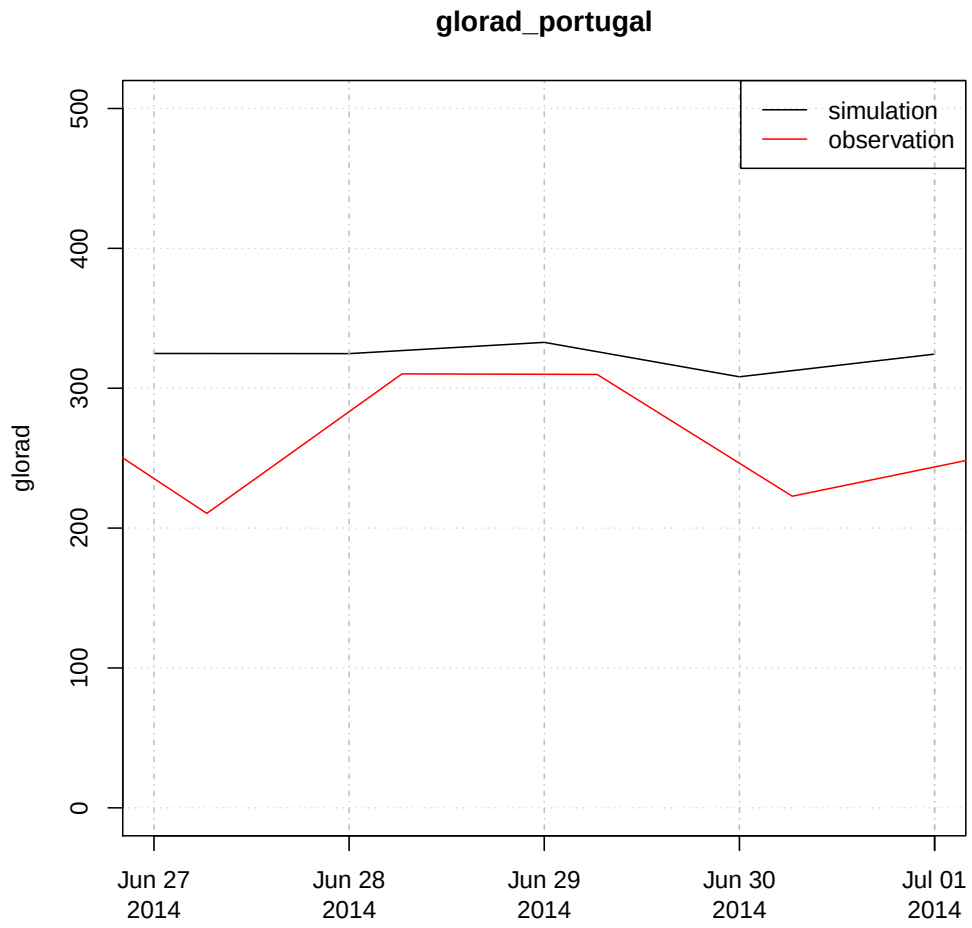

Figure 6.1: .

6.1.2 glorad: Morocco

6.2 Net incoming radiation rad_net

6.2.1 rad_net: Portugal

6.3 Soilheat flux soilheat

6.3.1 soilheat: Portugal

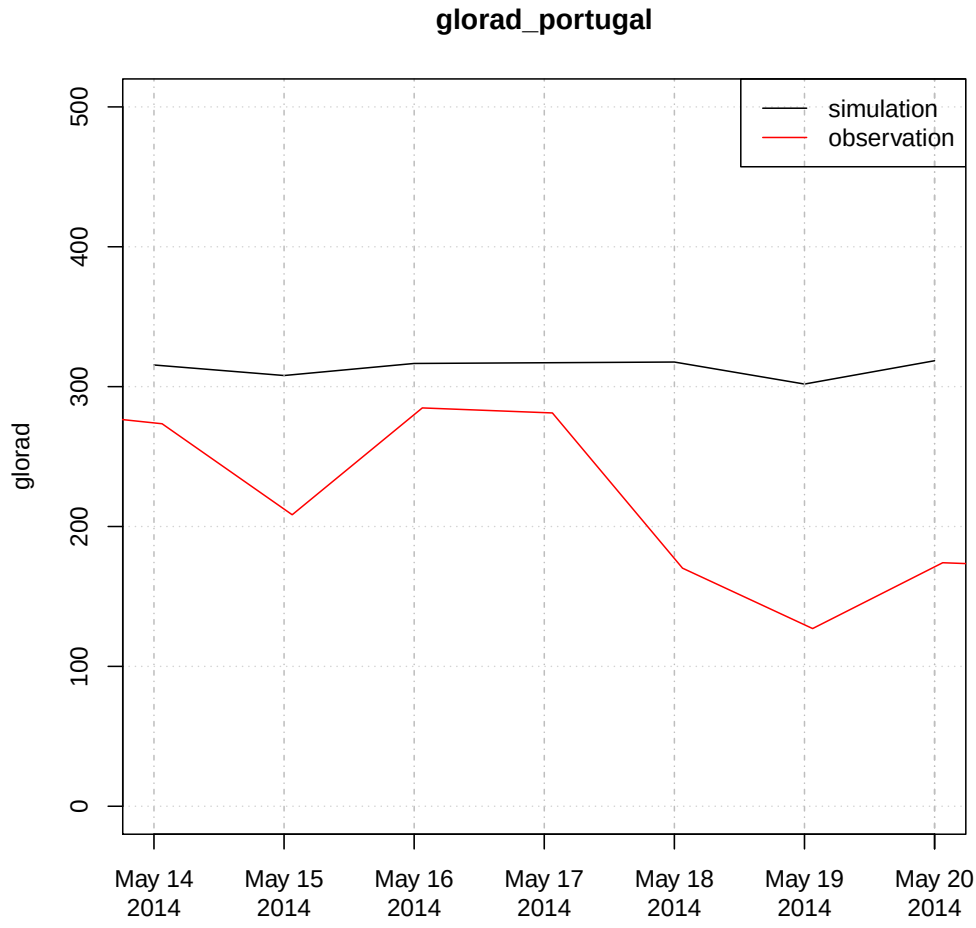
glorad_portugal
simulation
observation
glorad
0
100
200
300
400
500
May 14
2014
May 15
2014
May 16
2014
May 17
2014
May 18
2014
May 19
2014
May 20
2014

Figure 6.2: .

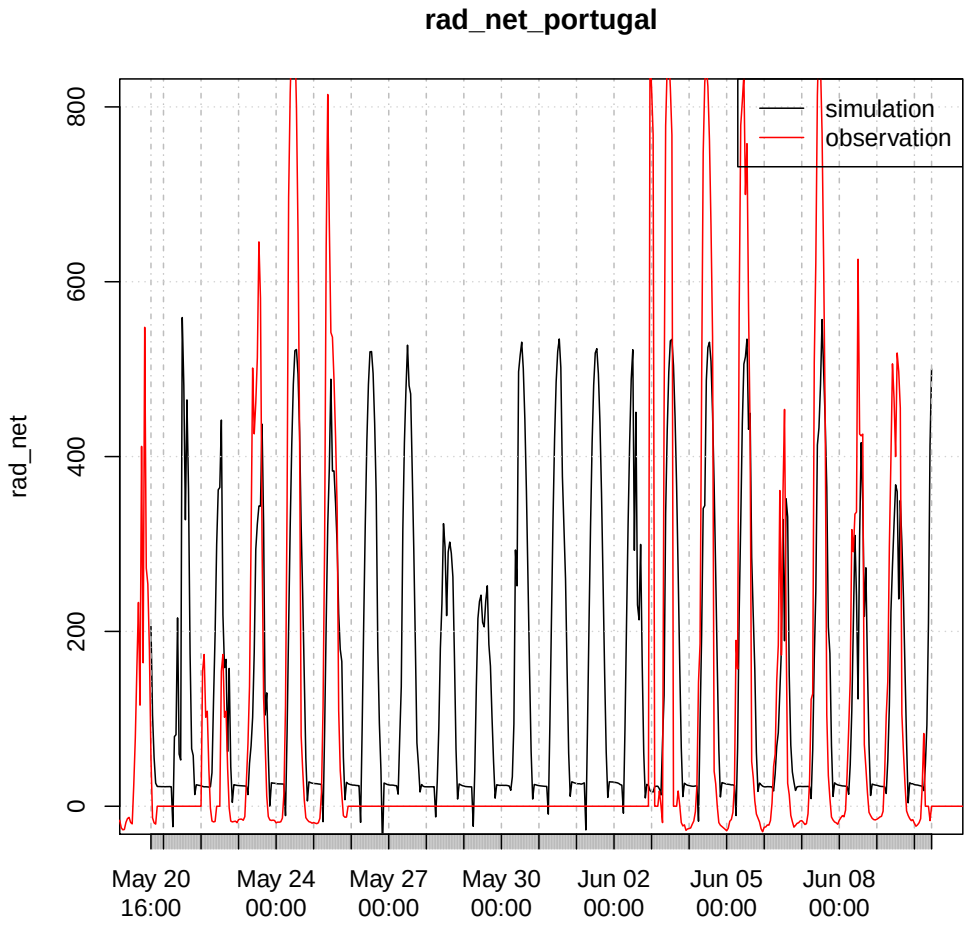
rad_net_portugal
rad_net
0
200
400
600
800
simulation
observation
May 20
16:00
May 24
00:00
May 27
00:00
May 30
00:00
Jun 02
00:00
Jun 05
00:00
Jun 08
00:00

Figure 6.3: .

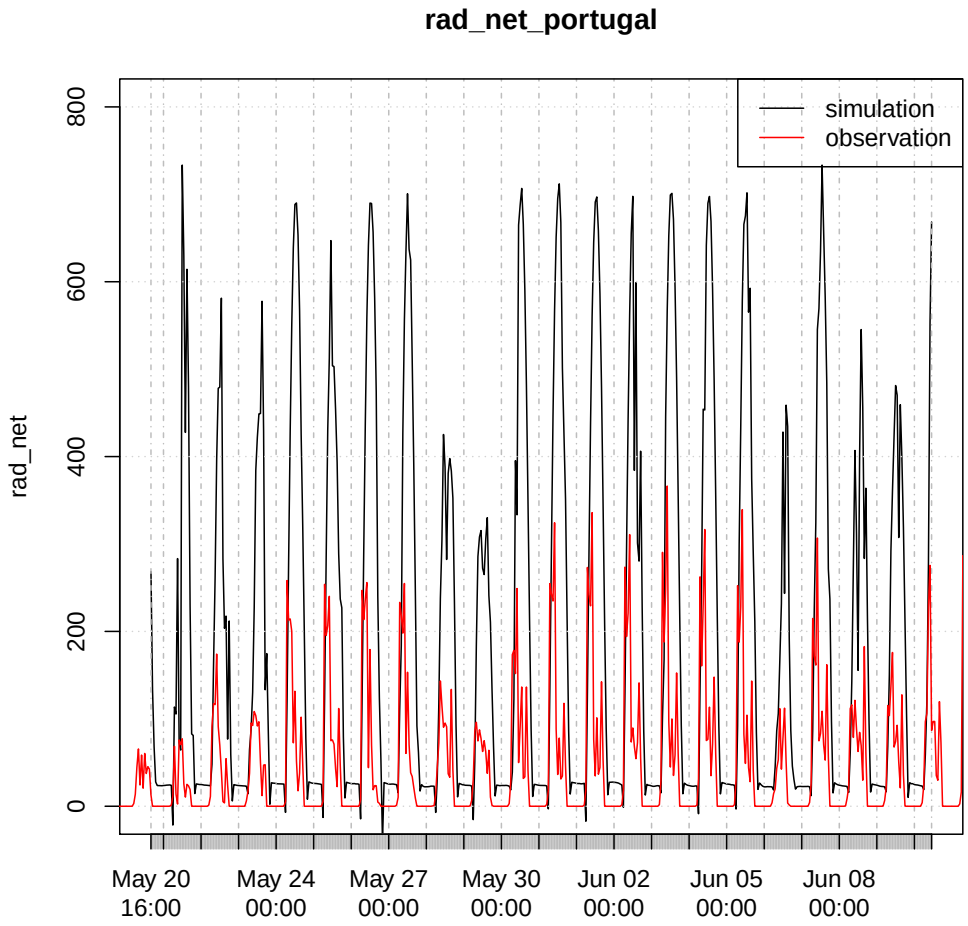
rad_net_portugal
simulation
observation
rad_net
0
200
400
600
800
May 20
16:00
May 24
00:00
May 27
00:00
May 30
00:00
Jun 02
00:00
Jun 05
00:00
Jun 08
00:00

Figure 6.4: .

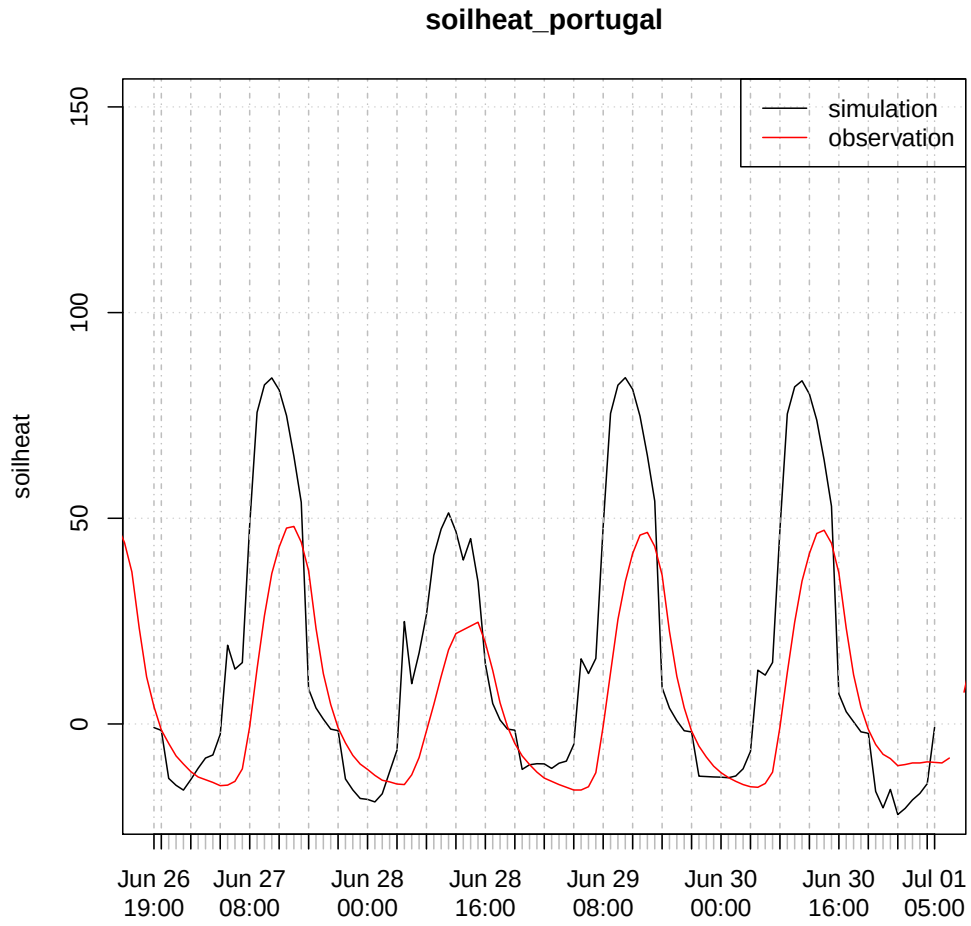
soilheat_portugal
simulation
observation
soilheat
0
50
100
150
Jun 26
19:00
Jun 27
08:00
Jun 28
00:00
Jun 28
16:00
Jun 29
08:00
Jun 30
00:00
Jun 30
16:00
Jul 01
05:00

Figure 6.5: .

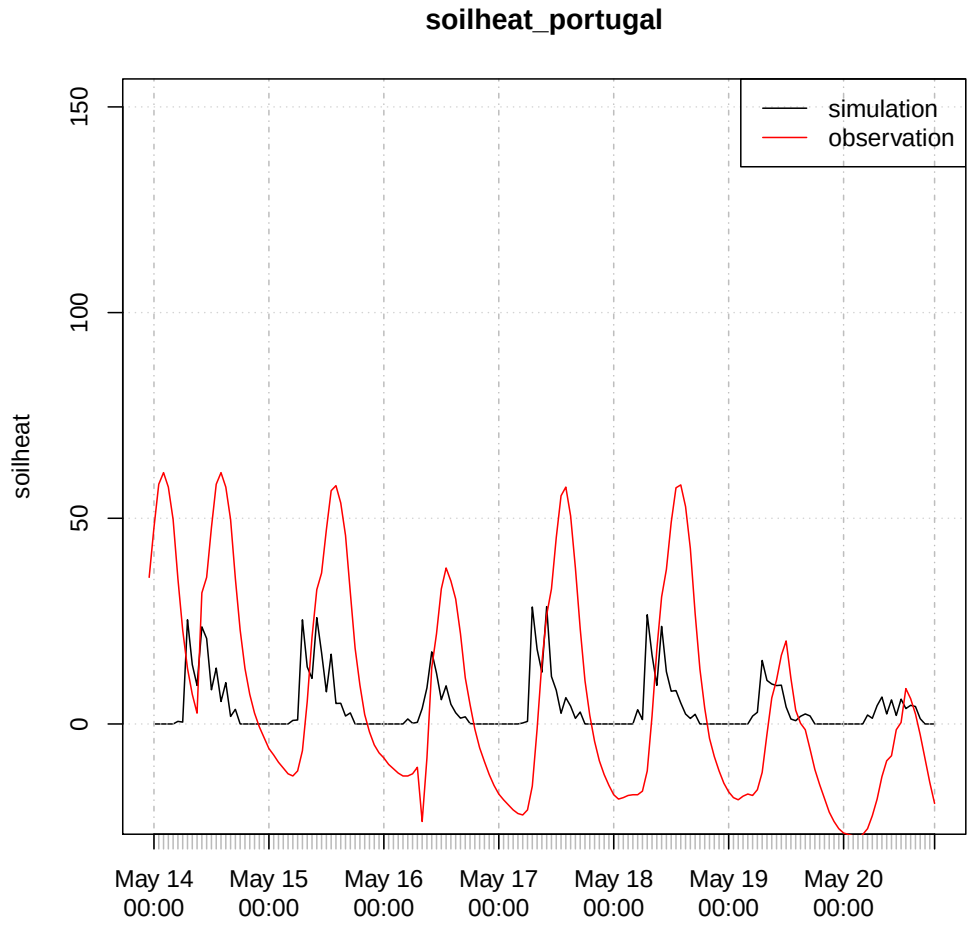
soilheat_portugal
simulation
observation
soilheat
0
50
100
150
May 14
00:00
May 15
00:00
May 16
00:00
May 17
00:00
May 18
00:00
May 19
00:00
May 20
00:00

Figure 6.6: .

7 Results: overview

7.1 Parameters

An overview of the parameters is given for the paramNum group (object-specific scalar parameters, HS Portugal: Tab. 7.1, NSA Portugal: Tab. 7.2, Morocco: Tab.), the sharedParamNum group (group-specific scalar parameters, HS Portugal: Tab. 7.3, NSA Portugal: Tab. 7.4, Morocco: Tab.), and the inputExt group (group-specific scalar parameters given as time series, HS Portugal: Tab. 7.5, NSA Portugal: Tab. 7.6, Morocco: Tab.).

Table 7.1: Object-specific scalar parameters (paramNum), HS Portugal

Parameter	Value	Unit	Comment
bubble	8.08	hPa	PTF by Rawls and Brakensiek (1985)
crop_faoref	1.00	–	evaporation of reference crop
crop_makk	0.80	–	Eq. (3.12)
elev	160.00	m	local elevation map
glo_half	200.00	W m^{-2}	guessed
lat	39.14		GIS data
lon	8.33		ditto
par_stressHum	0.03	hPa^{-1}	guessed
pores_ind	0.45	–	PTF by Rawls and Brakensiek (1985)
res_leaf_min	50.00	s m^{-1}	guessed
soil_dens	1500.00	kg m^{-3}	guessed
wc_etmax	0.13	–	calibration
wc_pwp	0.07	–	PTF by Rawls and Brakensiek (1985)
wc_res	0.05	–	(PTF by Rawls and Brakensiek (1985))
wc_sat	0.39	–	PTF by Wösten et al. (1999)
wstressmax	10.00	hPa	wilting point
wstressmin	1.00	hPa	field capacity

Table 7.2: Object-specific scalar parameters (paramNum), NSA Portugal

Parameter	Value	Unit	Comment
bubble	8.08	hPa	PTF by Rawls and Brakensiek (1985)
crop_faoref	1.00	–	evaporation of reference crop
crop_makk	0.80	–	Eq. 3.12
elev	160.00	m	local elevation map
glo_half	200.00	W m^{-2}	guessed
lat	39.14		GIS data
lon	8.33		ditto
par_stressHum	0.03	hPa^{-1}	guessed
pores_ind	0.45	–	PTF by Rawls and Brakensiek (1985)
res_leaf_min	50.00	s m^{-1}	guessed
soil_dens	1500.00	kg m^{-3}	guessed
wc_etmax	0.13	–	calibration
wc_pwp	0.07	–	PTF by Rawls and Brakensiek (1985)
wc_res	0.05	–	(PTF by Rawls and Brakensiek (1985))
wc_sat	0.39	–	PTF by Wösten et al. (1999)
wstressmax	10000.00	hPa	wilting point
wstressmin	100.00	hPa	field capacity

Table 7.3: Group-specific scalar parameters (sharedParamNum), HS Portugal

Parameter	Value	Unit	Comment
drag_coef	0.07	–	calibration
eddy_decay	2.50	–	as used by Shuttleworth and Wallace (1985) from Monteith (1973)
emis_a	0.34	–	as used by Maidment (1993) for average conditions
emis_b	-0.14	–	ditto
ext	0.40	–	guessed
f_day	0.14	–	estimation from soil heat data
f_night	0.52	–	ditto
fcorr_a	0.74	–	as used by Maidment (1993)
fcorr_b	0.26	–	ditto
h_humMeas	2.00	m	
h_tempMeas	2.00	m	
h_windMeas	2.00	m	
radex_a	0.22	–	estimation from radiation data
radex_b	0.78	–	ditto
res_b	25.00	s m^{-1}	as used by Shuttleworth and Wallace (1985)
rough_bare	0.01	m	ditto
rss_a	37.50	–	
rss_b	-1.23	–	

Table 7.4: Group-specific scalar parameters (sharedParamNum), NSA Portugal

Parameter	Value	Unit	Comment
drag_coef	0.07	–	calibration
eddy_decay	2.50	–	as used by Shuttleworth and Wallace (1985) from Monteith (1973)
emis_a	0.34	–	as used by Maidment (1993) for average conditions
emis_b	-0.14	–	ditto
ext	0.40	–	guessed
f_day	0.29	–	estimation from soil heat data
f_night	0.39	–	ditto
fcorr_a	1.35	–	as used by Maidment (1993)
fcorr_b	-0.35	–	ditto
h_humMeas	4.84	m	
h_tempMeas	4.84	m	
h_windMeas	4.84	m	
radex_a	0.14	–	estimation from radiation data
radex_b	0.67	–	ditto
res_b	25.00	s m^{-1}	as used by Shuttleworth and Wallace (1985)
rough_bare	0.01	m	ditto
rss_a	37.50	–	
rss_b	-1.23	–	

Table 7.5: Time-dependent parameters (inputExt), HS Portugal

Parameter	Value	Unit
alb	0.07	–
cano_height	0.20	m
lai	0.78	–

Table 7.6: Time-dependent parameters (inputExt), NSA Portugal

Parameter	Value	Unit
alb	0.30	–
cano_height	4.84	m
lai	1.40	–

8 Conclusion

– Soil heat flux needs a better model.

Bibliography

R.G. Allen, L.S. Pereira, D. Raes, and M. Smith. Crop evapotranspiration – guidelines for computing crop water requirements – FAO irrigation and drainage paper 56. Technical report, Food and Agriculture Organization of the United Nations, 1998. URL `http://www.fao.org/docrep/X0490E/x0490e00.htm`. Rome.

A. Berger. Le potentiel hydrique et la résistance à la diffusion dans les stomates indicateurs de l'état hydrique de la plante. In *Proceedings of the Uppsala Symposium, 1970*, pages 201–211. UNESCO, 1973. Paris.

D. Brunt. Notes on radiation in the atmosphere. *Quarterly Journal of the Royal Meteorological Society*, 58:389–418, 1932.

H.A.R. De Bruin. From Penman to Makkink. In *Hooghart, J.C. (Ed.), Evaporation and Weather: Proceedings and information No. 39*. TNO Committee on Hydrological Research, 1987. The Hague.

O.T. Denmead. Temperate cereals. In J.L. Monteith, editor, *Vegetation and the atmosphere, Vol. 2*, pages 1–31. Academic Press, 1976.

J. Doorenbos and W. O. Pruitt. Guidelines for predicting crop water requirements – FAO irrigation and drainage paper 24. Technical report, Food and Agriculture Organization of the United Nations, 1977. URL `http://www.fao.org/3/a-f2430e.pdf`. Rome.

E. Dufrêne. *Photosynthèse, consommation en eau et modélisation de la production chez le palmier à huile*. PhD thesis, Université Paris-Sud, Orsay, 1989.

R.A. Feddes. Crop factors in relation to makkink reference-crop evapotranspiration. In *Hooghart, J.C. (Ed.), Evaporation and Weather: Proceedings and information No. 39*. TNO Committee on Hydrological Research, 1987. The Hague.

A. Güntner. *Large-scale hydrological modelling in the semi-arid north-east of Brazil*. PhD thesis, Universität Potsdam, 2002.

S.B. Idso and R.D. Jackson. Thermal radiation from the atmosphere. *Journal of Geophysical Research*, 74(23):5397–5403, 1969.

O.L. Jahn. Penetration of photosynthetically active radiation as a measurement of canopy density of citrus trees. *Journal of the American Society for Horticultural Science*, 104(4):557–560, 1979.

P.G. Jarvis and J.I.L. Morison. The control of transpiration and photosynthesis by the stomata. In P.G. Jarvis and T.A. Mansfield, editors, *Stomatal Physiology (S.E.B. Sem. Vol. 8)*, pages 247–279. Cambridge University Press, London, 1981.

N. Katerji, A. Perrier, and A.K. Oulid-Aissa. Exploration au champ et interprétation de la variation horizontale et verticale de la résistance stomatique: cas d'une culture de luzerne (*Medicago sativa* l.). *Agronomie*, 3:847–856, 1983.

D. Kneis. A lightweight framework for rapid development of object-based hydrological model engines. *Environmental Modelling & Software*, 68:110–121, 2015.

T. Lohammar, S. Larsson, S. Linder, and S.O. Falk. Fast-simulation models of gaseous exchange in scots pine. In T. Persson, editor, *Structure and Function of Northern Coniferous Forests – An Ecosystem Study*. Ecol. Bull., 32:505–523, 1980.

K. Ludwig and M. Bremicker, editors. *The water balance model LARSIM – Design, content and application*, volume 22 of *Freiburger Schriften zur Hydrologie*. University of Freiburg, Institute of Hydrology, 2006.

D.R. Maidment, editor. *Handbook of Hydrology*. McGraw-Hill, Inc., 1993.

G.F. Makkink. Testing the Penman formula by means of lysimeters. *International Journal of Water Engineering*, 11:277–288, 1957.

T. Markvart and L. Castañer. *Practical Handbook of Photovoltaics*. Elsevier, 2003.

J.L. Monteith. Evaporation and environment. *Symposia of the Society for Experimental Biology*, 19: 205–224, 1965.

J.L. Monteith. *Principles of Environmental Physics*. Edward Arnold, 1st ed., 1973. London.

J.L. Monteith. *Principles of Environmental Physics*. Edward Arnold, 2nd ed., 1990. London.

K. Mroos. *Assessment of the soil water balance and irrigation recharge by combination of cosmic ray neutron sensing and eddy covariance technique on a citrus orchard in the Haouz plain, Morocco*. Universität Potsdam, 2014.

W.J. Rawls and D.L. Brakensiek. Prediction of soil water properties for hydrologic modeling. In *Proceedings of the Symposium on Watershed Management in the Eighties*, pages 293–299. ASCE, 1985. Denver, CO.

B. Saugier and N. Katerji. Some plant factors controlling evapotranspiration. *Agricultural and Forest Meteorology*, 54:263–277, 1991.

F. Scheffer and P. Schachtschabel. *Lehrbuch der Bodenkunde*. Spektrum Akademischer Verlag, 16th ed. edition, 2010. Heidelberg.

W.J. Shuttleworth. A one-dimensional theoretical description of the vegetation-atmosphere interaction. *Boundary-Layer Meteorology*, 10:273–302, 1976. doi: 10.1007/bf00919390.

W.J. Shuttleworth. Putting the 'vap' into evaporation. *Hydrology & Earth System Sciences*, 11(1): 210–244, 2007.

W.J. Shuttleworth and R.J. Gurney. The theoretical relationship between foliage temperature and canopy resistance in sparse crops. *Quarterly Journal of the Royal Meteorological Society*, 116: 497–519, 1990. doi: 10.1002/qj.49711649213.

W.J. Shuttleworth and J.S. Wallace. Evaporation from sparse crops – an energy combination theory. *Quarterly Journal of the Royal Meteorological Society*, 111:839–855, 1985. doi: 10.1002/qj.49711146910.

U. Sonnewald. Physiology of movement. In A. Bresinsky, C. Körner, J.W. Kadereit, G. Neuhaus, and U. Sonnewald, editors, *Strasburger's Plant Science*, pages 531–568. Springer, 2013.

G. Tetzlaff. Albedo of the Sahara. Technical report, University of Cologne, 1983.

Z. Uchijima. Maize and rice. In J.L. Monteith, editor, *Vegetation and the atmosphere, Vol. 2*, pages 1–31. Academic Press, 1976.

B. Warrit, J.J. Landsberg, and M.R. Thorpe. Response of apple leaf stomata to environmental factors. *Plant Cell Environment*, 3:13–22, 1980.

J.H.M. Wösten, A. Lilly, A. Nemes, and C. le Bas. Development and use of a database of hydraulic properties of european soils. *Geoderma*, 90(3–4):169–185, 1999.